Planta (2012) 235:311–323
DOI 10.1007/s00425-011-1508-7

ORIGINAL ARTICLE

AtPTR4 and AtPTR6 are differentially expressed, tonoplast-localized members of the peptide transporter/nitrate transporter 1 (PTR/NRT1) family

Annett Weichert · Christopher Brinkmann · Nataliya Y. Komarova · Daniela Dietrich · Kathrin Thor · Stefan Meier · Marianne Suter Grotemeyer · Doris Rentsch

Received: 9 May 2011 / Accepted: 12 August 2011 / Published online: 9 September 2011

Abstract Members of the peptide transporter/nitrate transporter 1 (PTR/NRT1) family in plants transport a variety of substrates like nitrate, di- and tripepetides, auxin and carboxylates. We isolated two members of this family from *Arabidopsis*, AtPTR4 and AtPTR6, which are highly homologous to the characterized di- and tripeptide transporters AtPTR1, AtPTR2 and AtPTR5. All known substrates of members of the PTR/NRT1 family were tested using heterologous expression in *Saccharomyces cerevisiae* mutants and oocytes of *Xenopus laevis*, but none could be identified as substrate of AtPTR4 or AtPTR6. *AtPTR4* and *AtPTR6* show distinct expression patterns, while *AtPTR4* is expressed in the vasculature of the plants, *AtPTR6* is highly expressed in pollen and during senescence. Phylogenetic analyses revealed that AtPTR2, 4 and 6 belong to one clade of subgoup II, whereas AtPTR1 and 5 are found in a second clade. Like AtPTR2, AtPTR4-GFP and AtPTR6-GFP fusion proteins are localized at the tonoplast. Vacuolar localization was corroborated by co-localization of AtPTR2-YFP with the tonoplast marker protein GFP-AtTIP2;1 and AtTIP1;1-GFP. This indicates that the two clades reflect different intracellular localization at the tonoplast (AtPTR2, 4, 6) and plasma membrane (AtPTR1, 5), respectively.

Keywords *Arabidopsis* · Dipeptide · Peptide · Tonoplast · Transport

Abbreviations

aa	Amino acid
GFP	Green fluorescent protein
GUS	*β*-Glucuronidase
N	Nitrogen
ORF	Open reading frame
YFP	Yellow fluorescent protein

Introduction

In plants, nitrogen (N) is an important nutrient for growth and yield. To secure their N supply plants evolved multiple transport systems for N uptake from the soil as well as for intra- and intercellular reallocation of N containing compounds. N can be taken up not only as inorganic N, i.e. nitrate and ammonium, but also as organic N, e.g. amino acids, small peptides or even protein (Wright 1962; Komarova et al. 2008; Paungfoo-Lonhienne et al. 2008; Näsholm et al. 2009; Tegeder and Rentsch 2010). Soil inorganic and organic N as well as root-derived organic N is transported via the xylem to source leaves and can be reallocated to sink tissues—mainly as organic N—via the phloem. A large number of data indicate that this reallocation of organic N takes place primarily in the form of amino acids and ureides, though small peptides may also contribute (Komarova et al. 2008; Tegeder and Rentsch 2010). Transport of organic N is important throughout the life cycle of plants, although translocation patterns may change dramatically.

A. Weichert · C. Brinkmann · N. Y. Komarova · D. Dietrich · K. Thor · S. Meier · M. Suter Grotemeyer · D. Rentsch (✉)
Institute of Plant Sciences, University of Bern, Altenbergrain 21, 3013 Bern, Switzerland
e-mail: doris.rentsch@ips.unibe.ch

D. Dietrich
Division of Plant and Crop Sciences, University of Nottingham, Sutton Bonington Campus, Loughborough LE12 5RD, UK

K. Thor
Institute of Agricultural and Nutritional Sciences, University of Halle-Wittenberg, Betty-Heimann-Strasse 3, 06120 Halle (Saale), Germany

Furthermore, surplus N can be stored long term and/or transiently in the vacuole, predominantly in the form of nitrate, amino acids and as vegetative or seed storage proteins (Marty 1999; Martinoia et al. 2007).

Besides organic N originating from direct uptake or assimilation of inorganic N, protein-degradation products contribute to the soluble organic N pool. Release of amino acids and peptides from protein degradation is supposed to play an important role during developmental stages with rapid proteolysis, i.e. during senescence and germination. Senescing leaves recycle most of their N, which is translocated to sink organs (Himelblau and Amasino 2001). Proteins of senescing chloroplasts are degraded by catabolic enzymes and the resulting breakdown products, i.e. peptides and amino acids (Hörtensteiner and Feller 2002), may subsequently be exported. During germination, seed storage proteins are degraded and products made available for the establishment of the seedling (Herman and Larkins 1999). It could be shown that in germinating barley (*Hordeum vulgare*) grains transport rates for di- and oligopeptides were higher than transport rates for amino acids, indicating that transport of peptides may play an important role during mobilization of storage proteins (Higgins and Payne 1978). Moreover, peptide transport was detected in mature broad bean (*Vicia fava*) leaves, suggesting a role of peptide translocation during all developmental stages (Jamaï et al. 1994).

Peptide transporters can be grouped in different families according to the length of the peptide recognized (Rentsch et al. 2007; Tsay et al. 2007). Di- and tripeptides are transported by members of the PTR/NRT1 (peptide transporter/nitrate transporter 1) family found in bacteria, fungi, plants and animals (Rentsch et al. 2007; Tsay et al. 2007). The PTR/NRT1 family can be divided into four subgroups and comprises more than 50 genes in *Arabidopsis thaliana*, while only few members per species are present in other kingdoms (Tsay et al. 2007). Besides peptides, plant members of the PTR/NRT1 family transport other substrates including nitrate, auxin or carboxylates, and it is assumed that additional substrates might be identified in the future (Tsay et al. 2007; Krouk et al. 2010). Di- and tripeptide transporters, which have been functionally characterized so far, were classified into two different subgroups. While *Arabidopsis* AtPTR1, 2 and 5 (Rentsch et al. 1995; Song et al. 1996; Dietrich et al. 2004; Komarova et al. 2008), faba bean VfPTR1 (Miranda et al. 2003), barley HvPTR1 (West et al. 1998), rice OsPTR6 (Ouyang et al. 2010) and *Hakea actites* HaPTR4 (Paungfoo-Lonhienne et al. 2009) belong to subgroup II (Fig. 1), AtPTR3 (Karim et al. 2007) is a member of subgroup III (Tsay et al. 2007). Up to now, the clade of AtPTR1-like and AtPTR2-like proteins contain only di- and tripeptide transporters, while transporters for other substrates were found in other clades of subfamily II (including AtNRT1.5, AtNRT1.8 and OsNRT1.1) or in other subfamilies (Tsay et al. 2007; Lin et al. 2008; Krouk et al. 2010; Li et al. 2010; Ouyang et al. 2010; Tegeder and Rentsch 2010).

Functional analyses showed that AtPTR1, AtPTR2 and AtPTR5 are high-affinity, low-selective transporters for di- and tripeptides when characterized in heterologous expression systems such as *Saccharomyces cerevisiae* mutants and *Xenopus laevis* oocytes (Rentsch et al. 1995; Chiang et al. 2004; Hammes et al. 2010). Chiang et al. (2004) also demonstrated that AtPTR2 transports peptides and protons by a random binding, simultaneous transport mechanism.

While AtPTR1, AtPTR5 and HvPTR1 were shown to be localized at the plasma membrane and thus function as cellular uptake systems (Waterworth et al. 2000; Dietrich et al. 2004; Komarova et al. 2008), proteome approaches identified AtPTR2 and a PTR2-homolog from barley in the tonoplast fraction (Carter et al. 2004; Shimaoka et al. 2004; Dunkley et al. 2006; Endler et al. 2006). Furthermore, *Hakea actites* HaPTR4/GFP fusion proteins were localized at the vacuolar membrane (Paungfoo-Lonhienne et al. 2009).

We studied two so far non-characterized *Arabidopsis* transporters of subgroup II, which are highly similar to AtPTR2. While being non-functional when expressed in heterologous expression systems, we show that these proteins are localized at the tonoplast, supporting the phylogenetic analyses that identified the *Arabidopsis* di- and tripeptide transporters in two different clades, reflecting distinct intracellular localization. Furthermore, tissue-specific expression indicates distinct roles in the plant.

Materials and methods

Plant cultivation and transformation

Arabidopsis thaliana L. plants (ecotype Columbia) (Col-0) were grown in soil or axenic culture using AM medium (2.16 g L^{-1} Murashige and Skoog (MS) salts [Duchefa, Haarlem, The Netherlands], 1% sucrose, pH 5.8, solidified with 0.7% BiTEK agar [BD Difco, Sparks, MO, USA]). Plants were cultivated in a growth chamber under long-day conditions with a photoperiod of 16 h light (150 µmol m^{-2} s^{-1}) and day/night temperatures of 22°C/18°C at 65%/60% relative humidity. Alternatively, plants were cultivated under short-day conditions 8 h light (120 µmol m^{-2} s^{-1})/16 h dark; 22°C/18°C; 65%/60% relative humidity.

Flowering *Arabidopsis* plants were transformed using the floral dip method (Clough and Bent 1998) by *Agrobacterium tumefaciens* (GV3101 pMP90)-mediated gene transfer (Koncz and Schell 1986) as described in Dietrich et al. (2004). Transgenic plants were selected using BASTA (150 mg L^{-1}; Hoechst Schering AgrEvo, Berlin, Germany).

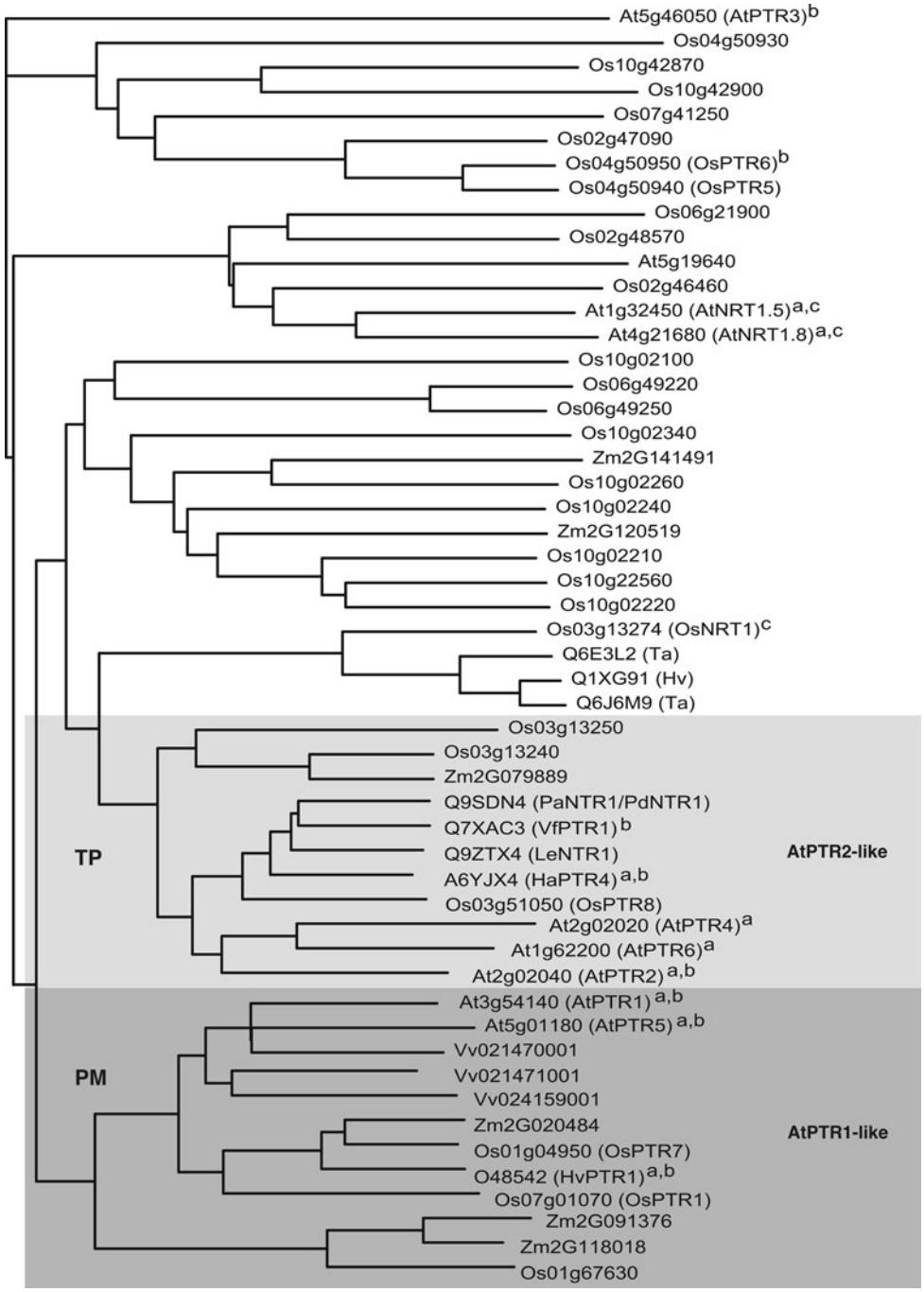

Fig. 1 Phylogenetic relationship of members of subgroup II of the PTR/NRT1 gene family. The analysis was performed using the aligned protein sequences of members of subgroup II of the PTR/NRT1 gene family (see Tsay et al. 2007). Subgroup II comprises the functionally characterized di- and tripeptide transporters AtPTR1 (At3g54140; Dietrich et al. 2004), AtPTR2 (At2g02040; Frommer et al. 1994; Rentsch et al. 1995; Song et al. 1996), AtPTR5 (At5g01180; Komarova et al. 2008), VfPTR1 (Miranda et al. 2003), HaPTR4 (Paungfoo-Lonhienne et al. 2009), HvPTR1 (West et al. 1998), and OsPTR6 (Ouyang et al. 2010) and the nitrate transporters AtNRT1.5 (Lin et al. 2008), AtNRT1.8 (Li et al. 2010) and OsNRT1.1 (Lin et al. 2000). AtPTR4 (At2g02020), AtPTR6 (At1g62200), PaPTR2 (Campalans et al. 2001), LeNTR1 (AF016713), OsPTR1, OsPTR4, OsPTR5, OsPTR7 and OsPTR8 (Ouyang et al. 2010) and several other genes from rice (Os), maize (Zm), wheat (Ta), barley (Hv) and grape (Vv) were also included. The protein sequences were aligned using ClustalX followed by Neighbour-Joining analysis in PAUP 4.0 to generate the tree (Swofford 2003). The phylogram was displayed using FigTree. AtPTR3 (At5g46050; Karim et al. 2007), a member of subgroup III was used as outgroup. Clades with AtPTR2-like and AtPTR1-like transporters are highlighted in light and dark grey, respectively. *TP* tonoplast, *PM* plasma membrane. AtNRT1.5 and AtNRT1.8 are also localized at the plasma membrane (Lin et al. 2008, 2010). [a]Subcellular localization of the protein was confirmed experimentally. [b]Functionally characterized di- and tripeptide transporters. [c]Functionally characterized nitrate transporters

DNA and RNA work

Standard methods (cloning, transformation of bacteria, plasmid preparation, and DNA cleavage with restriction enzymes, RNA isolation, RT-PCR) were performed as described by Ausubel et al. (1994) and Sambrook et al. (1989).

The ORF of *AtPTR4* (At2g02020) was amplified by RT-PCR using RNA of *A. thaliana* Col-0 seedlings and primers 5′-ATG GCT TCC ATT GAT GAA GAA AGG-3′, 5′-TCA AAC CTT CAT ATG AGT ATA TTT CAC-3′. For *AtPTR6* (ATG1) cDNA of *A. thaliana* Col-0 flowers was used and primers 5′-TAG TTT AAT TGG TAT ACT GGG CCA TC-3′, 5′-TTA CAA AGC CTT CTT CTT TGT GTG CT-3′. The PCR products were cloned into the *Sma*I site of the vector pDR196 (Rentsch et al. 1995). The *AtPTR6* (ATG2; At1g62200) cDNA was obtained from RIKEN BioResource Center (Koyadai, Tsukuba-shi, Japan; RAFL-09-09-B15; pda05229), cleaved with *Sfi*I and cloned into the corresponding site of the vector pDR201 (Rentsch, unpublished).

For expression in oocytes the *Spe*I/*Pst*I fragment containing the ORF of *AtPTR4* was transferred to vector pBF (Baukrowitz et al. 1999). The ORFs of *AtPTR6* (ATG1) and (ATG2) were amplified from respective pDR constructs with primers 5′-ATA ACT AGT ATG AGT TCC AGT AAT CTA TTT GC-3′, 5′-ATA AGA TCT TTA CAA AGC CTT CTT CTT TGT GTG-3′ and 5′-AAT ACT AGT ATG GTG AAT TCG AAT GAA GAA GAC-3′, 5′-ATA AGA TCT TTA CAA AGC CTT CTT CTT TGT GTG-3′, respectively. The resulting fragments were cleaved with *Spe*I and *Bgl*II and cloned into the corresponding pBF sites (Baukrowitz et al. 1999).

The promoters of *AtPTR4* (2621 bp) and *AtPTR6* (1739 bp) were amplified by PCR with primers (*AtPTR4*) 5′-GTC TTC TTT CAA CTT CGA ACT TTG-3′, 5′-TTT TTA CTT TCT CCT CAA CAT GAC-3′ and (*AtPTR6*) 5′-AAT ACT AGT GAG ATT GTG TTC CTA ATA TCA TTC C-3′, 5′-AAT CCC GGG ATT CTC CTT TCG TCT TCT TCA TTC G-3′, respectively, and *A. thaliana* Col-0 genomic DNA as template. The PCR fragment of the *AtPTR4* promoter was cloned into the *Sma*I-site of pBluescript SK (Stratagene, Amsterdam, The Netherlands). The construct was linearized with *Pst*I, blunt ended with T4 DNA polymerase followed by restriction with *Bam*HI. The resulting promoter fragment was cloned into the *BamHI*/*Sma*I sites of pCB308 (Xiang et al. 1999). The *AtPTR6* promoter fragment was cleaved with *Sma*I/*Spe*I and cloned into the corresponding sites of pCB308 (Xiang et al. 1999).

For translational fusions with GFP, the ORF was amplified by PCR and cloned in pUC18-spGFP6 and pUC18-GFP5Tsp for C and N-terminal fusion proteins (Suter and Rentsch, unpublished). AtPTR2-GFP fusion: primers 5′-CGA CTA GTA TGG GTT CCA TCG AAG AAG AAG-3′ and 5′-ATA GAT CTG ACG AAG CTT TCT TTT GCT TAT AC-3′, fragment cloned into the *Spe*I/*Bgl*II site. GFP-AtPTR2 fusion: primers 5′-CGA CTA GTA TGG GTT CCA TCG AAG AAG AAG-3′ and 5′-CAG TCG ACC TAC GAC GAA GCT TTC TTT TGC-3′, fragment cleaved with *Spe*I/*Sal*I and cloned into the *Nhe*I/*Sal*I site. AtPTR4-GFP fusion: primers 5′-CTA GGA TCC ATG GCT TCC ATT GAT GAA G-3′, 5′-CTA ACT AGT AAC CTT CAT ATG AGT ATA TTT C-3′, fragment cloned into the *Spe*I/*Bam*HI site. GFP-AtPTR4 fusion: primers 5′-CTA GCT AGC ATG GCT TCC ATT GAT GAA G-3′, 5′-CTA GTC GAC TCA AAC CTT CAT ATG AGT ATA-3′, fragment cloned into *Nhe*I/*Sal*I site. AtPTR6 (ATG2)-GFP fusion: primers 5′-CTA GCT AGC ATG GTG AAT TCG AAT GAA GAA GAC-3′, 5′-AAT AGA TCT TCC AAA GCC TTC TTC TTT GTG TGC-3′, cleaved with *Nhe*I/*Bgl*II and cloned into the *Spe*I/*Bgl*II site. GFP-AtPTR6 (ATG2) fusion: primers 5′-CTA GCT AGC ATG GTG AAT TCG AAT GAA GAA GAC-3′, 5′-AAT GTC GAC TTA CAA AGC CTT CTT CTT TGT GTG-3′, cloned into *Nhe*I/*Sal*I site. AtPTR6 (ATG1)-GFP fusion: 5′-CTA GCT AGC ATG AGT TCC AGT AAT CTA TTT GC-3′, 5′-AAT AGA TCT TCC AAA GCC TTC TTC TTT GTG TGC-3′ cleaved with *Nhe*I/*Bgl*II and cloned into the *Spe*I/*Bgl*II site. GFP-AtPTR6 (ATG1) fusion: 5′-CTA GCT AGC ATG AGT TCC AGT AAT CTA TTT GC-3′, 5′- AAT GTC GAC TTA CAA AGC CTT CTT CTT TGT GTG-3′ fragment cloned into *Nhe*I/*Sal*I site.

For translational fusion with EYFP pUC18-spEYFP was constructed using primers 5′-ACC GGC TAG CGC AAT GGT GAG CAA GG-3′ and 5′-TAT CTA GAT TAC TTG TAC AGC TCG TC-3′ to amplify the *EYFP* fragment from pEYFP-C1 (Clontech, Saint-Germain-en-Laye, France). The fragment was cleaved with *Nhe*I/*Xba*I and cloned into *Nhe*I/*Xba*I of pUC18-spGFP6 (Suter and Rentsch, unpublished results). *AtPTR2* was excised from pUC18-*AtPTR2*spGFP6 with *Spe*I/*Bgl*II and the *AtPTR2* fragment was transferred into the corresponding site of pUC18-spEYFP.

Sequence identity of all PCR-amplified fragments was verified by sequencing.

RT-PCR for determining length of *AtPTR4*: AtPTR4$\Delta^{866-901}$ was constructed using pUC18-AtPTR4-spGFP6 as template and primers 5′-CTA GGA TCC ATG GCT TCC ATT GAT GAA G-3′, 5′-ACG GGT TAG TGT TTG CAT CTC CTT CGT CCG TGG AGT CTT CAG GGA CCT TG-3′, 5′-CTA ACT AGT AAC CTT CAT ATG AGT ATA TTT C-3′, 5′-CAA GGT CCC TGA AGA CTC CAC GGA CGA AGG AGA TGC AAA CAC TAA CCC GT-3′. Equal amounts of these fragments were used for fusion PCR with primers 5′-CTA GGA TCC ATG GCT TCC ATT GAT GAA G-3′ and 5′-CTA ACT AGT AAC

CTT CAT ATG AGT ATA TTT C-3′. The resulting fragment was cleaved using *Bam*HI and *Spe*I and cloned into the *Bam*HI/*Spe*I sites of pUC18-spGFP6. pUC18-*AtPTR4*-spGFP6, pUC18-*AtPTR4*$\Delta^{866-901}$-spGFP6 and cDNA of Col-0 seedlings were used as templates for the PCR using primers 5′-TAC CGT GTT CAT GGG ACT TGC TAC TAT-3′ and 5′-CTT CCA CGG GTT AGT GTT TGC ATC TC-3′ to determine the length of the *AtPTR4* mRNA.

The 5′ RLM-RACE was performed twice each with RNA from flowers and senescent leaves of Col-0 plants. The reactions were carried out according to the manufacturer's instructions (Ambion LTD, Cambridgeshire, UK). For the first 5′ RLM-RACE the primer 5′-TCG CAA TAG AGA CTC CCA TAA ACA-3′ was used for the RT reactions and primers 5′-TGA AGC CGA GAG TGT CAA C-3′, 5′-GCT GAT GGC GAT GAA TGA ACA CTG-3′ for the first PCR, and 5′-CCT CGA GAA CGT CAC TAG CTG CAG A-3′, 5′-CGC GGA TCC GAA CAC TGC GTT TGC TGG CTT TGA TG-3′ for the second PCR. The resulting fragments were cleaved using *Xho*I and *BamH*I and cloned into the *Xho*I/*BamH*I sites of pBluescript SK (Stratagene). In the second experiment the RT reactions were performed with primer 5′-TGA AGC CGA GAG TGT CAA C-3′ and the first PCR using 5′-GCT GAT GGC GAT GAA TGA ACA CTG-3′, 5′-CCT CGA GAA CGT CAC TAG CTG CAG A-3′ and 5′-GAA TAA AGG GAC AAG CTT TCC AG-3′, 5′-CGC GGA TCC GAA CAC TGC GTT TGC TGG CTT TGA TG-3′ for the second PCR. The resulting fragments were cloned blunt ended into the *Sma*I site of pBluescript SK (Stratagene).

Transient expression in protoplasts

Tobacco (*Nicotiana tabacum* L. cv. SNN) protoplasts were isolated and transformed as described by Neuhaus and Boevink (2001) with the following modifications: The enzyme solution contained 0.6% (w/v) cellulase Onozuka R10 (Serva, Heidelberg, Germany), 0.2% (w/v) macerozyme R10 (Serva) and 0.4 M sucrose in K3. The pH of W5 was adjusted to pH 5.8 with KOH. 300 µl tobacco protoplasts [2×10^6 protoplasts ml^{-1}] resuspended in MMM were added to 10–20 µg plasmid DNA premixed with 20 µg denatured herring sperm DNA. Samples were not rinsed with W5. The PEG solution contained 40% (w/v) PEG 4000 (Merck, Darmstadt, Germany).

Arabidopsis protoplasts were isolated as described by Song et al. (2003) and subsequently transformed according to Abel and Theologis (1994).

18 to 24 h after transformation, images were obtained using a confocal laser microscope (Leica DM RXE equipped with a Leica TCS SP 2 confocal scanner, Leica, Wetzlar, Germany). GFP was excited with a wavelength of 488 nm and GFP emission was detected at 500–520 nm. Chlorophyll fluorescence was detected at 628–768 nm. For co-localization GFP and YFP fluorescence were sequentially scanned. The excitation wavelength for GFP was 488 nm and for YFP 514 nm. GFP emission was detected at 492-511 nm and YFP emission was detected at 545–590 nm. Chlorophyll auto-fluorescence was detected at 603–752 nm.

Staining for β-glucuronidase activity

The GUS-activity in transgenic *Arabidopsis* plants was histochemically localized as described before (Dietrich et al. 2004). Embedded plant material (in 3% agarose) was sectioned to 100 µm using a vibratome (Series 1000; The Vibratome Company, St. Louis, MO, USA). Pictures were taken using a microscope (Axioskop; Zeiss, Jena, Germany) equipped with an Axiocam camera (Zeiss) or a binocular (Nikon SMZ-U, Nikon, Japan) equipped with a digital camera (Foculus; NET GmbH, Finning, Germany).

Expression in *Saccharomyces cerevisiae* and *Xenopus laevis* oocytes

Saccharomyces cerevisiae strain LR2 (*MATa hip1-614 his4-401 can1 ino1 ura3-52 ptr2Δ::hisG*; Rentsch et al. 1995) was transformed according to Dohmen et al. (1991). To test for peptide transport activity, transformants were selected on SC medium containing 1 mM His-Ala or 5 mM histidine as sole source of the required amino acid histidine (Rentsch et al. 1995) or on minimal medium containing one of different dipeptides as sole N source (1 g L^{-1} Ala-Phe, Phe-Ala, Pro-Ala, and 0.2 g L^{-1} Arg-Glu) and 20 mg L^{-1} inositol as well as 200 µM histidine.

Preparation of oocytes, cRNA synthesis and injection and TEVC measurements were performed as described by Hammes et al. (2010). 1 mM Ala-Ala, 1 mM Ala-Lys, 1 mM Ala-Asp, 10 mM histidine, 10 mM nitrate, 10 mM malate and 100 µM auxin were tested as potential substrates at pH 5.5 and pH 7.5, and membrane potentials ranging from +20 mV to −100 mV.

Results

Functional analysis of AtPTR4 and AtPTR6

AtPTR4 (At2g02020) and *AtPTR6* (At1g62200) are members of subgroup II of the PTR/NRT1 family (Fig. 1; Tsay et al. 2007; Komarova et al. 2008). The genes encode proteins, which are 75% identical and closely related to AtPTR2, displaying 71 and 70% amino acid identity, respectively (Table 1). Their similarity to AtPTR1 and AtPTR5 is lower (55–57%). As expected from the

Table 1 Similarity of selected *Arabidopsis* PTR/NRT1 transporters

	AtPTR2	AtPTR3	AtPTR4	AtPTR5	AtPTR6
AtPTR1	61.0	45.4	56.6	74.2	57.2
AtPTR2		43.3	71.0	59.3	70.4
AtPTR3			43.6	43.8	42.8
AtPTR4				55.1	75.4
AtPTR5					56.5

Identity of AtPTR1 (570 aa; At3g54140), AtPTR2 (585 aa; At2g02040), AtPTR3 (582 aa; At5g46050), AtPTR4 (557 aa; At2g02020), AtPTR5 (570 aa; At5g01180) and AtPTR6 (590 aa; At1g62200) on amino acid level (in %). AtPTR6 corresponds to AtPTR6 (ATG2) and AtPTR4 corresponds to the ORF identified by RT-PCR. Sequence alignment and calculation of protein sequence identity were performed using MegAlign (DNASTAR© Lasergene 8) and Clustal W. The amino acid sequences of the entire ORFs were used for the analysis

phylogenetic analysis, AtPTR3, which belongs to subgroup III, shows low similarity to AtPTR4 and 6 (44 and 43% identity). ORFs of *AtPTR4* and *6* were amplified by RT-PCR using RNA from *Arabidopsis* (Col-0) seedlings or flowers, respectively. Sequencing revealed that the *AtPTR4*-ORF differed from the predicted sequence present in databases such as TAIR (Swarbreck et al. 2007). The isolated *AtPTR4*-ORF was 36 nucleotides longer due to additional 7 or 8 nucleotides at the 5′ end and 29 or 28 nucleotides, respectively, at the 3′ end of the fourth intron. In an independent RT-PCR again only the longer version could be amplified (data not shown); therefore, this isolated ORF was used in further experiments. The *AtPTR6* ORF may also differ from the predicted sequence (At1g62200; Swarbreck et al. 2007) as 5′ RACE revealed an additional ATG, which is in frame and 42 nucleotides upstream (not shown). A contamination with genomic DNA can be excluded since the first intron was not present in the amplified fragment. The longer cDNA (including 152 nt upstream of the predicted ATG) was rare and identified in different 5′ RACE experiments in one out of 17 analysed cDNAs. The 5′ UTR of all shorter cDNAs contained approximately 25 nt upstream of the predicted ATG. In subsequent experiments both ORFs were used, referred to as *AtPTR6* ATG1 for the longer ORF and *AtPTR6* ATG2 for the predicted ORF.

For several transporters of subgroup II functional di- and tripeptide transport was demonstrated when expressed in *Saccharomyces cerevisiae* mutants or *Xenopus laevis* oocytes (Rentsch et al. 1995; Song et al. 1996; West et al. 1998; Chiang et al. 2004; Dietrich et al. 2004; Komarova et al. 2008; Hammes et al. 2010; Ouyang et al. 2010). To test a role of AtPTR4 and AtPTR6 in peptide transport, the ORFs were expressed in the peptide transport-deficient and histidine auxotroph *S. cerevisiae* strain LR2 (Rentsch et al. 1995). However, unlike their homologs neither AtPTR4 nor AtPTR6 (ATG1 or ATG2) mediated growth on selective concentrations of His-Ala (1 mM), other dipeptides or histidine (5 mM, data not shown). Two electrode voltage clamp studies using *X. laevis* oocytes injected with cRNA of *AtPTR4* or *AtPTR6* (ATG1 or ATG2) did not reveal peptide-induced currents on addition of a mixture of dipeptides (1 mM Ala–Ala, 1 mM Ala-Lys, 1 mM Ala-Asp) to the bathing solution at pH 5.5 and pH 7.5, and membrane potentials ranging from +20 mV to −100 mV. Furthermore, histidine, which is transported with low affinity by some di- and tripeptide transporters as well as nitrate, auxin or malate, which were shown to be substrates of other PTR/NRT1 members, did not induce currents (Tsay et al. 2007; Krouk et al. 2010).

AtPTR2, AtPTR4 and AtPTR6 are localized at the tonoplast

To assess the intracellular localization of AtPTR2, AtPTR4 and AtPTR6, AtPTR/GFP fusion constructs were transiently expressed in tobacco protoplasts and the localization was analysed using confocal laser scanning microscopy. The C-terminal fusions of AtPTR2, AtPTR4 and AtPTR6 with GFP showed fluorescence at the tonoplast (Fig. 2a, e, i, m). The tonoplast localization was verified with AtPTR2-YFP co-localizing with the tonoplast marker proteins GFP-AtTIP2;1 and AtTIP1;1-GFP in *Arabidopsis* protoplasts (Fig. 3; AtTIP1;1-GFP not shown; Boursiac et al. 2005) in contrast to the control transiently expressing free YFP (Fig. 3b, c). The N-terminal fusion of GFP to AtPTR2 and AtPTR4 resulted in fluorescence at internal membranes or weaker fluorescence at the tonoplast, respectively (Fig. 2c, g). While GFP-AtPTR6 (ATG2) localized at vesicle-like structures (Fig. 2k), GFP-AtPTR6 (ATG1) showed tonoplast localization (Fig. 2o). As control, free GFP in the cytosol (Fig. 2r) and the plasma membrane-localized AtPTR1-GFP (Fig. 2t) are also shown. These results confirmed the localization of AtPTR2 at the vacuolar membrane as inferred from proteome analyses (Carter et al. 2004; Shimaoka et al. 2004; Dunkley et al. 2006; Endler et al. 2006) and demonstrated that the closely related AtPTR4 and AtPTR6 are tonoplast proteins as well. Since previous studies showed that AtPTR1 and AtPTR5 are localized at the plasma membrane (Dietrich et al. 2004; Komarova et al. 2008), the results indicate that the two clades of the AtPTR1-like and AtPTR2-like proteins of subgroup II of the PTR/NRT1 family reflect different intracellular localizations (Fig. 1).

AtPTR4 and *AtPTR6* are differentially expressed in *Arabidopsis*

To determine the tissue-specific expression of *AtPTR4* and *AtPTR6* during plant development, transgenic plants

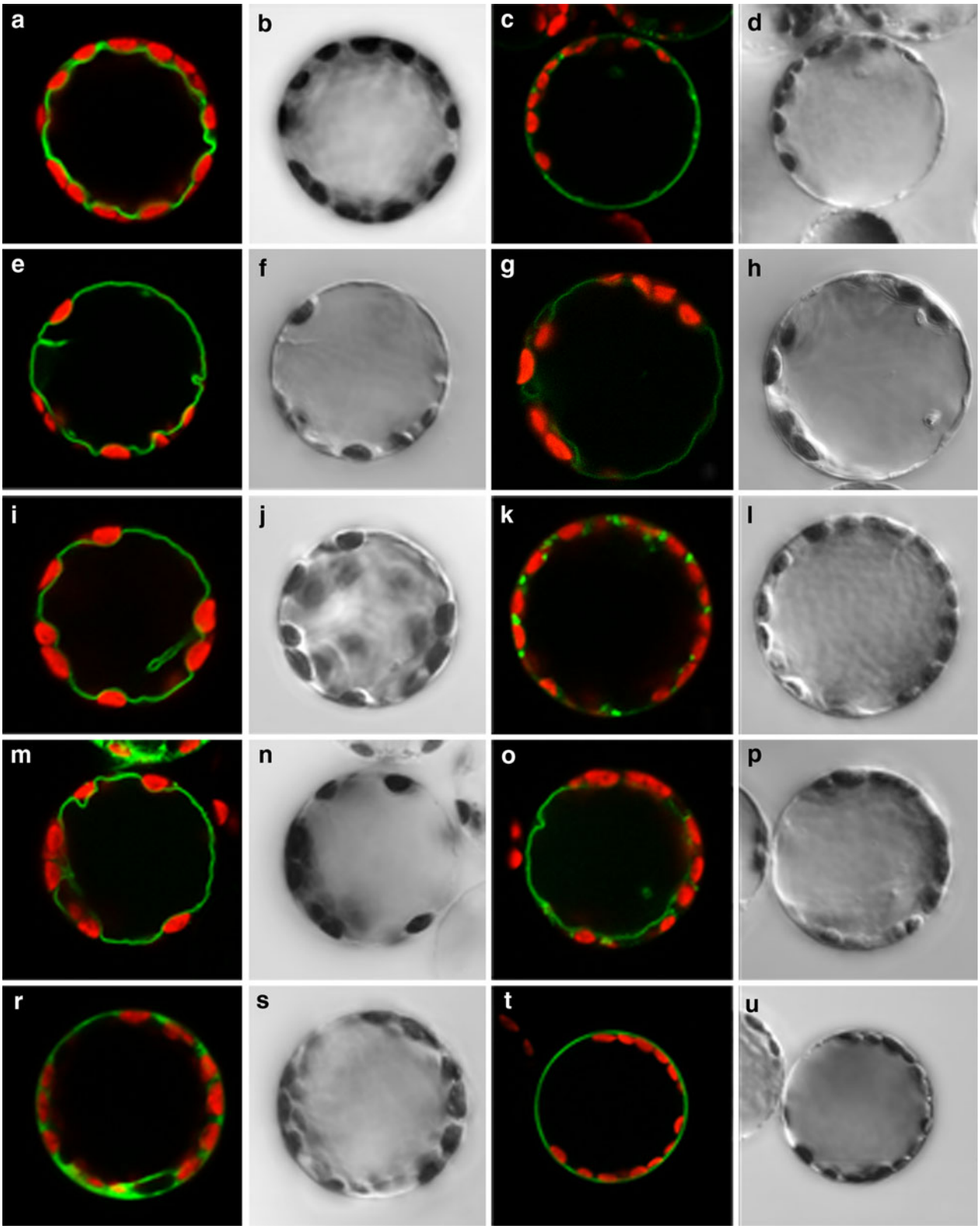

Fig. 2 Localization of AtPTR2/GFP, AtPTR4/GFP and AtPTR6/GFP fusion proteins at the tonoplast of tobacco protoplasts. Confocal laser-scanning microscope images (**a**, **c**, **e**, **g**, **i**, **k**, **m**, **o**, **r**, **t**) and corresponding bright-field images (**b**, **d**, **f**, **h**, **j**, **l**, **n**, **p**, **s**, **u**) of tobacco protoplasts transiently expressing fusion proteins of AtPTR/GFP or GFP alone. **a**, **b** AtPTR2-GFP. **c**, **d** GFP-AtPTR2. **e**, **f** AtPTR4-GFP. **g**, **h** GFP-AtPTR4. **i**, **j** AtPTR6-GFP (ATG2). **k**, **l** GFP-AtPTR6 (ATG2). **m**, **n** AtPTR6-GFP (ATG1). **o**, **p** GFP-AtPTR6 (ATG1). **r**, **s** free GFP. **t**, **u** AtPTR1-GFP. Merged images show GFP fluorescence (*green*) and chlorophyll fluorescence (*red*). Diameter of protoplasts is approximately 40 μm

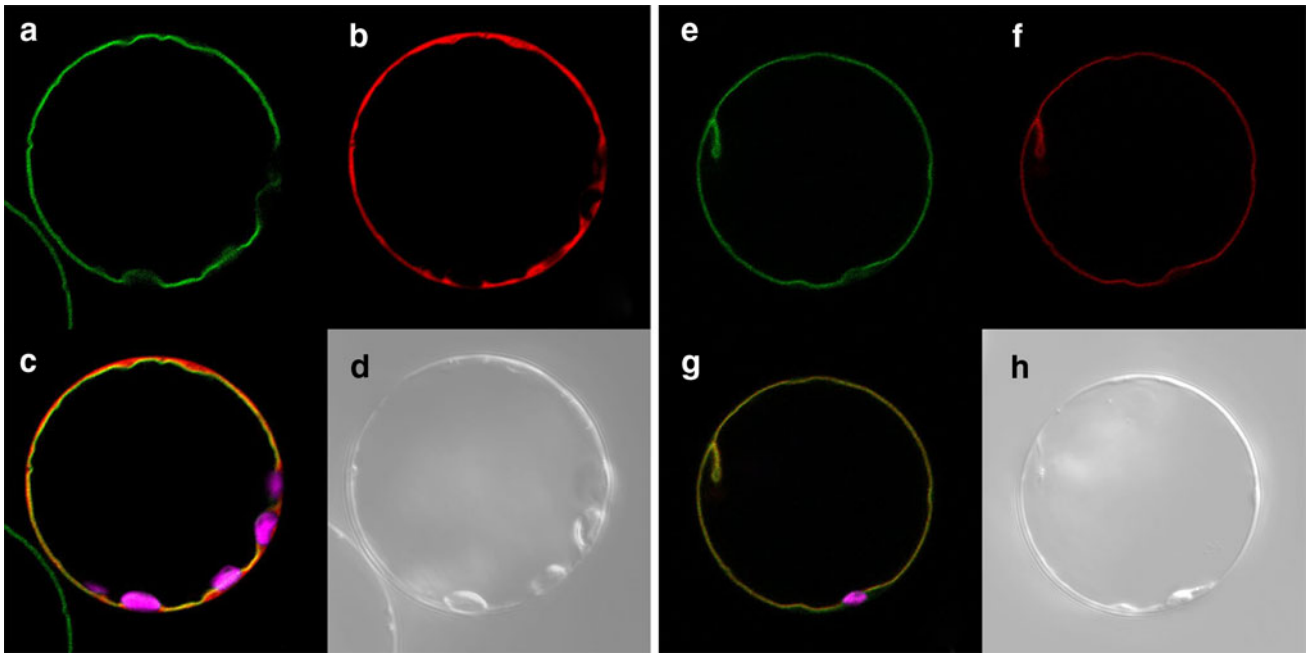

Fig. 3 Co-localization of the tonoplast marker GFP-AtTIP2;1 with AtPTR2-YFP or YFP. Confocal laser scanning microscopy images (**a–c** and **e–g**) and corresponding bright field images (**d**, **h**). **a–d** *Arabidopsis* protoplasts of 35S-GFP-AtTIP2;1 plants transiently expressing YFP. **e–h** *Arabidopsis* protoplasts of 35S-GFP-AtTIP2;1 plants transiently expressing AtPTR2-YFP. Merged images (**c**, **g**) show overlay of *green* (GFP fluorescence) and *red* (YFP fluorescence) in *yellow* and chlorophyll fluorescence (*magenta*). Diameter of protoplasts is approximately 35 µm

expressing the β-glucuronidase reporter gene under control of the *AtPTR4* or *AtPTR6* promoter were generated. Analyses of 33 independent lines of *AtPTR4-GUS* plants and 18 independent lines of *AtPTR6-GUS* plants showed comparable patterns of expression of 94 and 80%, respectively, and slightly varying intensities. *AtPTR4* promoter-GUS lines showed GUS-activity in roots (Fig. 4a, d–f), emerging lateral roots (Fig. 4f) and vasculature of leaves (Fig. 4a, b). Cross sections of leaves and roots revealed GUS activity in the central cylinder of roots (Fig. 4e) and the phloem and/or phloem parenchyma cells of leaf vasculature (Fig. 4c). Consistent with these findings, microarray analyses revealed highest *AtPTR4* mRNA levels in seedlings and leaves, except senescing leaves, and in phloem of roots (Winter et al. 2007; Hruz et al. 2008). Microarray data showed low expression levels for siliques corroborated by GUS staining of silique veins (not shown; Winter et al. 2007; Hruz et al. 2008). Furthermore, *AtPTR4-GUS* plants had no GUS-activity in pollen, which is supported by microarray data (Winter et al. 2007; Hruz et al. 2008).

AtPTR6-GUS plants showed GUS staining in roots of axenic (Fig. 5a, e) and soil-grown plants (Fig. 5f); in leaves, expression was highest in the vascular tissue (Fig. 5a, f). Strong GUS activity was detected in senescing leaves (Fig. 5g, h) and in pollen and pollen tubes (Fig. 5b–d). In agreement with these results, microarray data showed highest *AtPTR6* transcript levels in senescent leaves and pollen (Winter et al. 2007; Hruz et al. 2008), whereas strong GUS staining of roots was not found in the microarray analyses (Winter et al. 2007; Hruz et al. 2008). In microarray studies, *AtPTR6* mRNA could also be detected in petals, sepals and stamen of flower stage 15 though *AtPTR6* transcript levels were lower than in pollen or senescing leaves (Winter et al. 2007), whereas only three *AtPTR6-GUS* lines showed staining of the vasculature of petals and anthers (not shown).

Contrary to *AtPTR2*, *AtPTR4* and *6* could not be detected by Northern blot analyses indicating lower expression. Though levels of expression of different genes in microarray analyses cannot be directly compared, data from microarray analyses are consistent with these findings as the maxima of the expression levels of *AtPTR4* and *6* are much lower compared with *AtPTR2* (16- and twofold, respectively) with the highest expression in the root phloem for *AtPTR4*, in senescent leaves for *AtPTR6*, and imbibed seeds for *AtPTR2*. In contrast to *AtPTR2*, for *AtPTR4* and *AtPTR6* only low mRNA levels were reported in imbibed seeds (Winter et al. 2007; Hruz et al. 2008).

Discussion

To secure sufficient N supply throughout the plant, reduced N has to be transported between organelles, cells and over

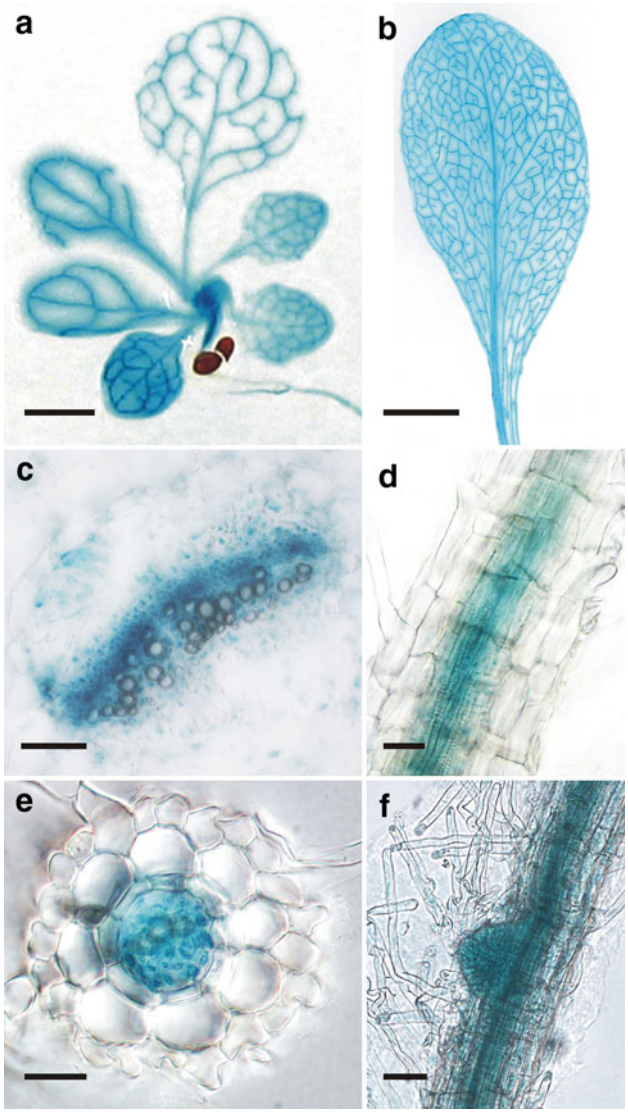

Fig. 4 Tissue specific expression of *AtPTR4*. *AtPTR4*-GUS activity in a 14-day-old seedling (**a**), rosette leaf (**b**), cross section of a leaf (**c**), longitudinal section of a root (**d**, **f**) and cross section of a root (**e**). *Scale bars* 2 mm (**a**), 10 mm (**b**), 25 μm (**c**–**e**), 100 μm (**f**)

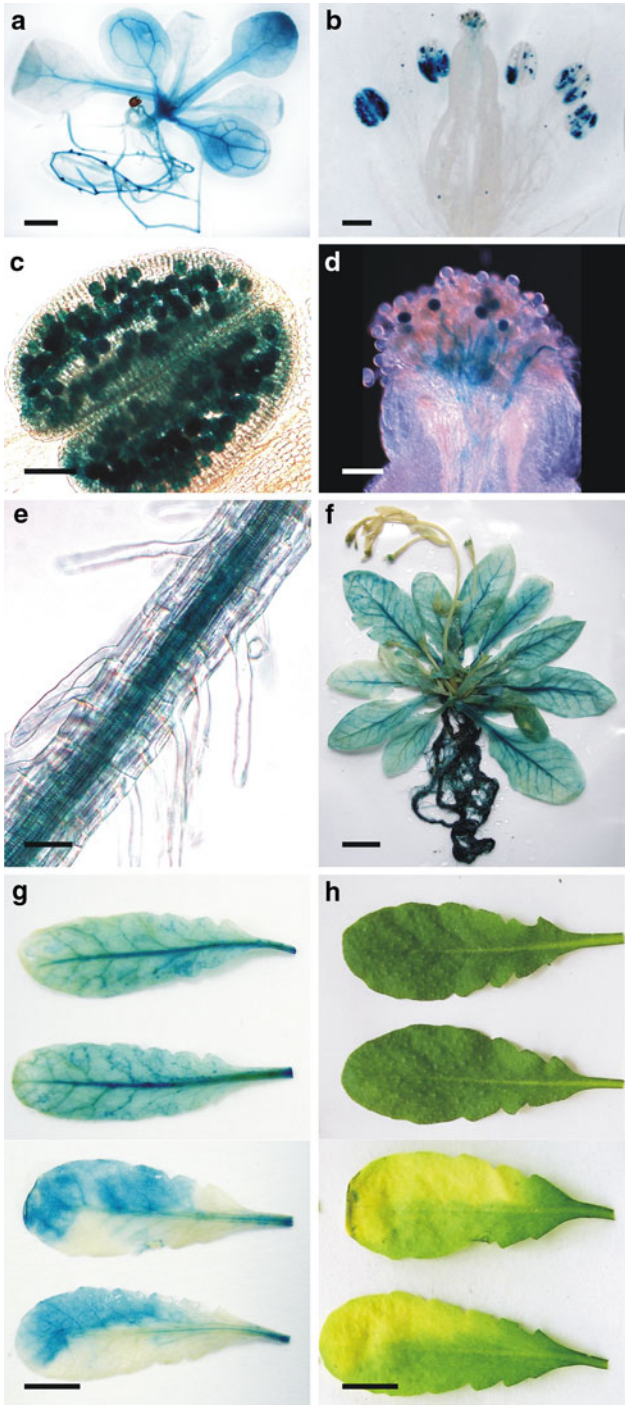

Fig. 5 GUS activity under the control of the *AtPTR6* promoter. GUS-staining of 2-week-old seedling (**a**), flower (**b**), anther with pollen (**c**), stigma with germinating pollen (**d**), lateral root of a 2-week-old seedling (**e**), soil-grown 7-week-old plant (**f**), GUS activity in leaves (**g**) before induction of senescence (*upper two rows*) and 6 days after dark induced senescence (*lower two rows*). **h** Leaves before staining are shown to indicate stage of senescence. *Scale bars* 2 mm (**a**), 500 μm (**b**), 100 μm (**c**–**e**), 15 mm (**f**), 10 mm (**g**, **h**)

long distances. N reallocation is especially high during germination and senescence. Though concentrations of peptides are largely unknown, it has been suggested that transport of peptides might be more efficient than transport of amino acids at these developmental stages (Higgins and Payne 1982). Using RT-PCR two members of the subgroup II of the PTR/NRT1-family, *AtPTR4* and *AtPTR6,* were isolated. Sequence comparisons showed a high (70–71%) amino acid identity to AtPTR2. The alignment of the *AtPTR4* ORF with publicly available sequence information (Schwacke et al. 2003; Swarbreck et al. 2007) revealed a difference of 36 nucleotides, indicating that the splicing sites of the fourth intron have been predicted incorrectly. Using primers flanking the region in question, the presence of the longer mRNA in *Arabidopsis* seedlings was verified. Furthermore, AtPTR6 might contain 14 additional amino acids at the N-terminus, as 5′ RACE identified a cDNA

with 152 nt upstream of the predicted ATG (ATG2) including an ATG (ATG1) which is in frame. Consistent with cDNA predictions the shorter cDNA contained only approximately 25 nt as 5′ UTR. The shorter cDNAs were more abundant indicating that the ORF starting at ATG2 might be predominantly translated. This is underpinned by the nucleotides near the translation initiation site of ATG2, containing 6 of 10 possible consensus nucleotides, whereas ATG1 contains none (Alexandrov et al. 2006). Also, a length of 25 nt of the 5′UTR is sufficient for initiation of translation (Mignone et al. 2002; Alexandrov et al. 2006). Whether in planta ATG1 and ATG2 are both used as start of translation remains to be further investigated.

C-terminal GFP-fusion proteins revealed that AtPTR2, AtPTR4 and AtPTR6 are localized at the vacuolar membrane. Tonoplast localization was corroborated by the co-localization of AtPTR2-YFP with the tonoplast intrinsic proteins GFP-AtTIP2;1 and AtTIP1;1-GFP in *Arabidopsis* protoplasts (Fig. 3). N-terminal fusions of GFP to AtPTR2, 4 and 6 resulted in fluorescence at the tonoplast, and/or localization at internal membranes and vesicle-like structures (Fig. 2). Incomplete targeting was also observed for GFP-HaPTR12, a plasma membrane localized protein belonging to subgroup III (Paungfoo-Lonhienne et al. 2009). Proteome studies reported AtPTR2 in the vacuolar membrane fraction (Carter et al. 2004; Dunkley et al. 2006) and showed tonoplast localization using transient expression of AtPTR2-GFP in tobacco epidermis cells (Dunkley et al. 2006), supporting the results of the C-terminal GFP fusion. AtPTR4 and AtPTR6 were not detected in these proteome studies, which is probably due to the much lower expression of *AtPTR4* and *AtPTR6* compared with *AtPTR2* (Winter et al. 2007; Hruz et al. 2008) and due to expression in different tissues (see below). The difference in intracellular localization of the AtPTR1-like and AtPTR2-like proteins of subgroup II at the plasma membrane (AtPTR1, 5) or tonoplast (AtPTR2, 4, 6) is mirrored by the phylogenetic analyses, assigning them to two clades (Fig. 1; Dietrich et al. 2004; Komarova et al. 2008). Localization of members of these clades from other plants strengthens this interpretation, as barley HvPTR1 was localized at the plasma membrane using affinity labelling (Waterworth et al. 2000), whereas *Hakea actites* HaPTR4 was demonstrated to be tonoplast-localized (Paungfoo-Lonhienne et al. 2009). Based on these findings we would suggest that proteins which are grouped with AtPTR2 are localized at the tonoplast, whereas those grouping with AtPTR1 are localized at the plasma membrane.

Plants generally possess more PTR/NRT1 genes than prokaryotes, fungi or animals; *Arabidopsis,* for instance, has 53 genes in four subgroups (Tsay et al. 2007). So far, all characterized members of the PTR/NRT1 family in *Arabidopsis* transport N-containing compounds, i.e. transport of nitrate, auxin and di- and tripeptides (Tsay et al. 2007; Krouk et al. 2010) have been reported. Transport of dicarboxylates has been shown for AgDCAT1, a member of the PTR/NRT1 family in alder (*Alnus glutinosa*) (Jeong et al. 2004). Thus, PTR/NRT1 members might transport a broad spectrum of possible substrates in plants. AtPTR2 was shown to be a high-affinity, highly selective H^+/di- and tripeptide co-transporter in heterologous systems such as *S. cerevisiae* mutants and *X. laevis* oocytes (Rentsch et al. 1995; Chiang et al. 2004); however, its localization at the tonoplast suggests a role in the export of small peptides from the vacuole in planta.

Although high sequence identity to AtPTR2 indicated that AtPTR4 and 6 are also di- and tripeptide transporters, functional di- or tripeptide transport could not be demonstrated using expression in *S cerevisiae* and *X. laevis* oocytes. Also uptake of histidine, which is transported by some di- and tripeptide transporters (Yamashita et al. 1997; Tegeder and Rentsch 2010) and transport of nitrate, malate and auxin (Jeong et al. 2004; Tsay et al. 2007; Krouk et al. 2010), which are substrates of more distantly related plant PTR/NRT1 members, could not be measured.

So far all functionally characterized members of the AtPTR2-clade of subgroup II, i.e. HaPTR4, AtPTR2 as well as VfPTR1 (Fig. 1) transport di- and tripeptides, even those that have been localized at the tonoplast (i.e. AtPTR2 and HaPTR4). With functional assays dependent on cellular uptake, partial mis-targeting of AtPTR2 or HaPTR4 to the plasma membrane in heterologous systems may have allowed identification of the substrates. Failure to detect dipeptide transport for AtPTR4 and 6 was perhaps due to a more stringent tonoplast localization in the heterologous expression systems and other approaches will have to be found to study their functional properties. However, the possibility that AtPTR4 and 6 transport substrates not tested so far cannot be excluded at the moment.

Analysis of the expression of *AtPTR4* using transgenic *Arabidopsis* plants expressing the *β*-glucuronidase gene under the control of the *AtPTR4* promoter showed highest expression in the central cylinder of roots and the phloem of leaves (Fig. 4), which is corroborated by microarray data (Winter et al. 2007; Hruz et al. 2008). Interestingly, *AtPTR4* is not expressed during stages of rapid mobilization of storage compounds, like senescence and germination, indicating that AtPTR4 is active throughout development. In contrast, the analysis of *AtPTR6-GUS* plants showed highest expression in senescing leaves and pollen (Fig. 5). These results are supported by microarray data (Winter et al. 2007; Hruz et al. 2008), which show that both *AtPTR6* and *AtPTR2* are induced during senescence (Winter et al. 2007; Hruz et al. 2008). Senescence is a highly organized process leading to the mobilization of N,

carbon (C) and minerals from the senescing leaf to sink organs (Buchanan-Wollaston 1997). While the substrate of AtPTR6 remains to be determined, AtPTR2 might be involved in the rapid translocation of breakdown products originating from mesophyll chloroplasts, which contain up to 75% of cellular N in C3-plants (Hörtensteiner and Feller 2002). Proteins are degraded by proteolytic enzymes, e.g. cystein proteases, which play an essential role not only during senescence, but also during programmed cell death and accumulation or mobilization of storage proteins (Palma et al. 2002; Grudkowska and Zagdanska 2004). Parrott et al. (2007) showed that 50 protease genes were upregulated during senescence in barley leaves including vacuole-localized thiol and serine proteases and thereby underpinning the role of the vacuole for protein turnover.

During seed germination, both the plasma membrane-localized *AtPTR1* and the tonoplast *AtPTR2* are highly expressed (Rentsch et al. 1995; Song et al. 1996; Dietrich et al. 2004; Winter et al. 2007) and may play a role in mobilizing peptides originating from degradation of storage proteins, similar to what was suggested for germinating barley grains (Higgins and Payne 1982; West et al. 1998).

Like *AtPTR5*, *AtPTR6* is highly expressed in pollen and pollen tubes. The plasma membrane-localized AtPTR5 was shown to facilitate dipeptide uptake into germinating pollen (Komarova et al. 2008). On the other hand, AtPTR6 could mediate release of stored compounds from the vacuole to the cytosol to deliver nutritional components for pollen tube growth. Transcriptome studies of germinating pollen also identified elevated transcript levels of members of the amino acid/auxin permease (AAAP) family and the oligopeptide transporter (OPT) family (Bock et al. 2006; Wang et al. 2008) supporting a role for N supply in pollen nutrition during germination and tube growth. Furthermore, Wang et al. (2008) observed no changes in ammonium and nitrate transport during pollen germination and pollen tube growth, but an increase in amino acid transport. This suggests that as during seed germination, transport of organic N is preferred in pollen development and germination processes. Though expression analyses indicated distinct roles in planta, so far analyses of knockout mutants did not reveal phenotypic changes or altered C or N allocation.

The vacuole is an organelle with a variety of specialized functions, e.g. turgor maintenance, transient storage of nutrients (inorganic and organic N), deposition of toxic compounds and storage of secondary metabolites (Martinoia et al. 2007). It also contains a number of hydrolytic activities and has a major function in recycling of amino acids (Müntz 2007). Schnell-Ramos et al. (2011) showed that large peptides of 9-27 amino acids, which may represent degradation products generated by the proteasome, are imported into barley vacuoles in a manner suggestive of the presence of an ABC-type transporter mediating long-chain peptide uptake for final degradation in the vacuole. The localization of AtPTR2 at the tonoplast and the transport mechanism described for AtPTR2 (Chiang et al. 2004) indicate that di- and tripeptides may subsequently be exported to the cytosol. Similarly, AtPTR4 and 6 may function in export of vacuolar storage compounds. Their expression patterns during germination (AtPTR2), senescence (AtPTR2, AtPTR6), pollen germination (AtPTR6) and in the vasculature (AtPTR4) reflect the various vacuolar functions as long-term and transient storage compartment.

Acknowledgments We wish to thank Erwin Sigel and Matthias Hediger (University of Bern) for providing *Xenopus* oocytes, Christophe Maurel (INRA/Montpellier) for providing AtTIP1;1-GFP and GFP-AtTIP2;1 plants and John M. Ward (University of Minnesota) for help with the phylogenetic analysis. This work was supported by grants from the Swiss National Science Foundation 3100A0–107507 and 31003A_127340, and EU Marie Curie Research Training Network 'VaTEP—Vacuolar Transport Equipment for Growth Regulation of Plants' (MRTN-CT-2006-035833).

References

Abel S, Theologis A (1994) Transient transformation of *Arabidopsis* leaf protoplasts: a versatile experimental system to study gene expression. Plant J 5:421–427

Alexandrov NN, Troukhan ME, Brover VV, Tatarinova T, Flavell RB, Feldmann KA (2006) Features of *Arabidopsis* genes and genome discovered using full-length cDNAs. Plant Mol Biol 60:69–85

Ausubel F, Brent R, Kingston R, Moore D, Seidman J, Smith J, Struhl K (1994) Current protocols in molecular biology. Wiley, New York

Baukrowitz T, Tucker SJ, Schulte U, Benndorf K, Ruppersberg JP, Fakler B (1999) Inward rectification in KATP channels: a pH switch in the pore. EMBO J 18:847–853

Bock KW, Honys D, Ward JM, Padmanaban S, Nawrocki EP, Hirschi KD, Twell D, Sze H (2006) Integrating membrane transport with male gametophyte development and function through transcriptomics. Plant Physiol 140:1151–1168

Boursiac Y, Chen S, Luu DT, Sorieul M, Van Den Dries N, Maurel C (2005) Early effects of salinity on water transport in *Arabidopsis* roots. Molecular and cellular features of aquaporin expression. Plant Physiol 139:790–805

Buchanan-Wollaston V (1997) The molecular biology of leaf senescence. J Exp Bot 48:181–199

Campalans A, Pages M, Messeguer R (2001) Identification of differentially expressed genes by the cDNA-AFLP technique during dehydration of almond (*Prunus amygdalus*). Tree Physiol 21:633–643

Carter C, Pan SQ, Jan ZH, Avila EL, Girke T, Raikhel NV (2004) The vegetative vacuole proteome of *Arabidopsis thaliana* reveals predicted and unexpected proteins. Plant Cell 16:3285–3303

Chiang CS, Stacey G, Tsay YF (2004) Mechanisms and functional properties of two peptide transporters, AtPTR2 and fPTR2. J Biol Chem 279:30150–30157

Clough SJ, Bent AF (1998) Floral dip: a simplified method for *Agrobacterium*-mediated transformation of *Arabidopsis thaliana*. Plant J 16:735–743

Dietrich D, Hammes U, Thor K, Suter Grotemeyer M, Flückiger R, Slusarenko AJ, Ward JM, Rentsch D (2004) AtPTR1, a plasma

membrane peptide transporter expressed during seed germination and in vascular tissue of *Arabidopsis*. Plant J 40:488–499
Dohmen RJ, Strasser AW, Honer CB, Hollenberg CP (1991) An efficient transformation procedure enabling long-term storage of competent cells of various yeast genera. Yeast 7:691–692
Dunkley TPJ, Hester S, Shadforth IP, Runions J, Weimar T, Hanton SL, Griffin JL, Bessant C, Brandizzi F, Hawes C, Watson RB, Dupree P, Lilley KS (2006) Mapping the *Arabidopsis* organelle proteome. Proc Natl Acad Sci USA 103:6518–6523
Endler A, Meyer S, Schelbert S, Schneider T, Weschke W, Peters SW, Keller F, Baginsky S, Martinoia E, Schmidt UG (2006) Identification of a vacuolar sucrose transporter in barley and Arabidopsis mesophyll cells by a tonoplast proteomic approach. Plant Physiol 141:196–207
Frommer WB, Hummel S, Rentsch D (1994) Cloning of an *Arabidopsis* histidine transporting protein related to nitrate and peptide transporters. FEBS Lett 347:185–189
Grudkowska M, Zagdanska B (2004) Multifunctional role of plant cysteine proteinases. Acta Biochim Pol 51:609–624
Hammes UZ, Meier S, Dietrich D, Ward JM, Rentsch D (2010) Functional properties of the *Arabidopsis* peptide transporters AtPTR1 and AtPTR5. J Biol Chem 285:39710–39717
Herman EM, Larkins BA (1999) Protein storage bodies and vacuoles. Plant Cell 11:601
Higgins CF, Payne JW (1978) Peptide transport by germinating barley embryos: uptake of physiological di- and tripeptides. Planta 138:211–215
Higgins CF, Payne JW (1982) Plant peptides. In: Boulter D, Parthier B (eds) Nucleic acids and proteins in plants. Encyclopedia of plant physiology. Springer, Berlin, pp 438–458
Himelblau E, Amasino RM (2001) Nutrients mobilized from leaves of *Arabidopsis thaliana* during leaf senescence. J Plant Physiol 158:1317–1323
Hörtensteiner S, Feller U (2002) Nitrogen metabolism and remobilization during senescence. J Exp Bot 53:927–937
Hruz T, Laule O, Szabo G, Wessendorp F, Bleuler S, Oertle L, Widmayer P, Gruissem W, Zimmermann P (2008) Genevestigator V3: a reference expression database for the meta-analysis of transcriptomes. Adv Bioinformatics 2008:420747
Jamaï A, Chollet JF, Delrot S (1994) Proton-peptide co-transport in broad bean leaf tissues. Plant Physiol 106:1023–1031
Jeong JY, Suh S, Guan CH, Tsay YF, Moran N, Oh CJ, An CS, Demchenko KN, Pawlowski K, Lee Y (2004) A nodule-specific dicarboxylate transporter from alder is a member of the peptide transporter family. Plant Physiol 134:969–978
Karim S, Holmstrom KO, Mandal A, Dahl P, Hohmann S, Brader G, Palva ET, Pirhonen M (2007) AtPTR3, a wound-induced peptide transporter needed for defence against virulent bacterial pathogens in *Arabidopsis*. Planta 225:1431–1445
Komarova NY, Thor K, Gubler A, Meier S, Dietrich D, Weichert A, Grotemeyer Suter M, Tegeder M, Rentsch D (2008) AtPTR1 and AtPTR5 transport dipeptides in planta. Plant Physiol 148:856–869
Koncz C, Schell J (1986) The promoter of Tl-DNA gene 5 controls the tissue-specific expression of chimeric genes carried by a novel type of *Agrobacterium* binary vector. Mol Gen Genet 204:383–396
Krouk G, Lacombe B, Bielach A, Perrine-Walker F, Malinska K, Mounier E, Hoyerova K, Tillard P, Leon S, Ljung K (2010) Nitrate-regulated auxin transport by NRT1.1 defines a mechanism for nutrient sensing in plants. Dev Cell 18:927–937
Li JY, Fu YL, Pike SM, Bao J, Tian W, Zhang Y, Chen CZ, Zhang Y, Li HM, Huang J, Li LG, Schroeder JI, Gassmann W, Gong JM (2010) The *Arabidopsis* nitrate transporter NRT1.8 functions in nitrate removal from the xylem sap and mediates cadmium tolerance. Plant Cell 22:1633–1646
Lin CM, Koh S, Stacey G, Yu SM, Lin TY, Tsay YF (2000) Cloning and functional characterization of a constitutively expressed nitrate transporter gene, *OsNRT1*, from rice. Plant Physiol 122:379–388
Lin SH, Kuo HF, Canivenc Gv, Lin CS, Lepetit M, Hsu PK, Tillard P, Lin HL, Wang YY, Tsai CB, Gojon A, Tsay YF (2008) Mutation of the Arabidopsis NRT1.5 nitrate transporter causes defective root-to-shoot nitrate transport. Plant Cell 20:2514–2528
Martinoia E, Maeshima M, Neuhaus HE (2007) Vacuolar transporters and their essential role in plant metabolism. J Exp Bot 58:83–102
Marty F (1999) Plant vacuoles. Plant Cell 11:587–600
Mignone F, Gissi C, Liuni S, Pesole G (2002) Untranslated regions of mRNAs. Genome Biol 3:1-0004.0010
Miranda M, Borisjuk L, Tewes A, Dietrich D, Rentsch D, Weber H, Wobus U (2003) Peptide and amino acid transporters are differentially regulated during seed development and germination in faba bean. Plant Physiol 132:1950–1960
Müntz K (2007) Protein dynamics and proteolysis in plant vacuoles. J Exp Bot 58:2391–2407
Näsholm T, Kielland K, Ganeteg U (2009) Uptake of organic nitrogen by plants. New Phytol 182:31–48
Neuhaus JM, Boevink P (2001) The green fluorescent protein (GFP) as reporter in plant cells. In: Hawes CR, Satiat-Jeunemaitre B (eds) Plant cell biology. Oxford University Press, Oxford, pp 127–142
Ouyang J, Cai Z, Xia K, Wang Y, Duan J, Zhang M (2010) Identification and analysis of eight peptide transporter homologs in rice. Plant Sci 179:374–382
Palma JM, Sandalio LM, Javier Corpas F, Romero-Puertas MC, McCarthy I, del Rìo LA (2002) Plant proteases, protein degradation, and oxidative stress: role of peroxisomes. Plant Physiol Biochem 40:521–530
Parrott DL, McInnerney K, Feller U, Fischer AM (2007) Steam-girdling of barley (*Hordeum vulgare*) leaves leads to carbohydrate accumulation and accelerated leaf senescence, facilitating transcriptomic analysis of senescence-associated genes. New Phytol 176:56–69
Paungfoo-Lonhienne C, Lonhienne TGA, Rentsch D, Robinson N, Christie M, Webb RI, Gamage HK, Carroll BJ, Schenk PM, Schmidt S (2008) Plants can use protein as a nitrogen source without assistance from other organisms. Proc Natl Acad Sci USA 105:4524–4529
Paungfoo-Lonhienne C, Schenk PM, Lonhienne TGA, Brackin R, Meier S, Rentsch D, Schmidt S (2009) Nitrogen affects cluster root formation and expression of putative peptide transporters. J Exp Bot 60:2665–2676
Rentsch D, Laloi M, Rouhara I, Schmelzer E, Delrot S, Frommer WB (1995) *NTR1* encodes a high affinity oligopeptide transporter in *Arabidopsis*. FEBS Lett 370:264–268
Rentsch D, Schmidt S, Tegeder M (2007) Transporters for uptake and allocation of organic nitrogen compounds in plants. FEBS Lett 581:2281–2289
Sambrook J, Fritsch EF, Maniatis T (1989) Molecular cloning: a laboratory manual, 2nd edn. Cold Spring Harbor Laboratory Press, New York
Schnell Ramos M, Abele R, Nagy R, Suter Grotemeyer M, Tampe R, Rentsch D, Martinoia E (2011) Characterization of a transport activity for long-chain peptides in barley mesophyll vacuoles. J Exp Bot 62:2403–2410
Schwacke R, Schneider A, van der Graaff E, Fischer K, Catoni E, Desimone M, Frommer WB, Flügge UI, Kunze R (2003) ARAMEMNON, a novel database for Arabidopsis integral membrane proteins. Plant Physiol 131:16–26
Shimaoka T, Ohnishi M, Sazuka T, Mitsuhashi N, Hara-Nishimura I, Shimazaki KI, Maeshima M, Yokota A, Tomizawa KI, Mimura T (2004) Isolation of intact vacuoles and proteomic analysis of

tonoplast from suspension-cultured cells of *Arabidopsis thaliana*. Plant Cell Physiol 45:672–683

Song W, Steiner HY, Zhang L, Naider F, Stacey G, Becker JM (1996) Cloning of a second Arabidopsis peptide transport gene. Plant Physiol 110:171–178

Song WY, Sohn EJ, Martinoia E, Lee YJ, Yang YY, Jasinski M, Forestier C, Hwang I, Lee Y (2003) Engineering tolerance and accumulation of lead and cadmium in transgenic plants. Nat Biotechnol 21:914–919

Swarbreck D, Wilks C, Lamesch P, Berardini TZ, Garcia-Hernandez M, Foerster H, Li D, Meyer T, Muller R, Ploetz L, Radenbaugh A, Singh S, Swing V, Tissier C, Zhang P, Huala E (2007) The Arabidopsis Information Resource (TAIR): gene structure and function annotation. Nucleic Acids Res 36:D1009–D1014

Swofford DL (2003) PAUP*. Phylogenetic analysis using parsimony (* and other methods). Sinauer Associates, Sunderland, Massachusetts

Tegeder M, Rentsch D (2010) Uptake and partitioning of amino acids and peptides. Mol Plant 3:997–1011

Tsay YF, Chiu CC, Tsai CB, Ho CH, Hsu PK (2007) Nitrate transporters and peptide transporters. FEBS Lett 581:2290–2300

Wang Y, Zhang WZ, Song LF, Zou JJ, Su Z, Wu WH (2008) Transcriptome analyses show changes in gene expression to accompany pollen germination and tube growth in Arabidopsis. Plant Physiol 148:1201–1211

Waterworth WM, West CE, Bray CM (2000) The barley scutellar peptide transporter: biochemical characterization and localization to the plasma membrane. J Exp Bot 51:1201–1209

West CE, Waterworth WM, Stephens SM, Smith CP, Bray CM (1998) Cloning and functional characterisation of a peptide transporter expressed in the scutellum of barley grain during the early stages of germination. Plant J 15:221–229

Winter D, Vinegar B, Nahal H, Ammar R, Wilson GV, Provart NJ (2007) An "electronic fluorescent pictograph" browser for exploring and analyzing large-scale biological data sets. PLoS ONE 2:e718

Wright DE (1962) Amino acid uptake by plant roots. Arch Biochem Biophys 97:174–180

Xiang C, Han P, Lutziger I, Wang K, Oliver DJ (1999) A mini binary vector series for plant transformation. Plant Mol Biol 40:711–717

Yamashita T, Shimada S, Guo W, Sato K, Kohmura E, Hayakawa T, Takagi T, Tohyama M (1997) Cloning and functional expression of a brain peptide/histidine transporter. J Biol Chem 272:10205–10211